AD-A177 374

SRI International

AFOSR-TR- 87-0100

per RJB

Annual Report   *February 1987*

15 MAY 85 to 14 NOV 86

GENERATION OF TENUOUS PLASMA CLOUDS IN THE EARTH'S ATMOSPHERE

By: ROBERT J. VIDMAR

Prepared for:

AIR FORCE OFFICE OF SCIENTIFIC RESEARCH
DIRECTORATE OF PHYSICAL AND GEOPHYSICAL SCIENCES
AFOSR/NP, BUILDING 410
BOLLING AIR FORCE BASE
WASHINGTON, DC   20332-6448

Approved by:

TAYLOR W. WASHBURN, *Director*
Remote Measurements Laboratory

LAWRENCE E. SWEENEY, JR., *Vice President*
System Technology Division

DTIC FILE COPY

87   2   20   216

4/77374

REPORT DOCUMENTATION PAGE

1a. REPORT SECURITY CLASSIFICATION UNCLASSIFIED		1b. RESTRICTIVE MARKINGS		
2a. SECURITY CLASSIFICATION AUTHORITY		3. DISTRIBUTION/AVAILABILITY OF REPORT Approved for public release; distribution is unlimited		
2b. DECLASSIFICATION/DOWNGRADING SCHEDULE N/A since unclassified				
4. PERFORMING ORGANIZATION REPORT NUMBER(S) SRI Project 8656		5. MONITORING ORGANIZATION REPORT NUMBER(S) **AFOSR·TR· 87-0100**		
6a. NAME OF PERFORMING ORGANIZATION SRI International	6b. OFFICE SYMBOL *(if applicable)*	7a. NAME OF MONITORING ORGANIZATION USAF, AFOSR		
6c. ADDRESS *(City, State, and ZIP Code)* 333 Ravenswood Avenue Menlo Park, CA 94025-3434		7b. ADDRESS *(City, State, and ZIP Code)* Bldg 410 Bolling AFB, D.C. 20332-6448		
8a. NAME OF FUNDING/SPONSORING ORGANIZATION USAF, AFSC Air Force Office of Scientific Res.	8b. OFFICE SYMBOL *(if applicable)* NP	9. PROCUREMENT INSTRUMENT IDENTIFICATION NUMBER F49620-85-K-0013		
8c. ADDRESS *(City, State, and ZIP Code)* Bldg. 410 Bolling AFB, D.C. 20332-6448		10. SOURCE OF FUNDING NUMBERS		

PROGRAM ELEMENT NO. 61102F	PROJECT NO. 2301	TASK NO. A8	WORK UNIT ACCESSION NO.

11. TITLE *(Include Security Classification)*

"Generation of Tenuous Plasma Clouds in the Earth's Atmosphere" (U)

12. PERSONAL AUTHOR(S)
Vidmar, Robert Joseph

13a. TYPE OF REPORT Annual	13b. TIME COVERED 86-11-14 FROM 85-5-15 TO 87-1-30	14. DATE OF REPORT *(Year, Month, Day)* 1987 February 6	15. PAGE COUNT 48

16. SUPPLEMENTARY NOTATION
This work was sponsored by AFOSR/NP under contract number F49620-85-K-0013.

17.	COSATI CODES		18. SUBJECT TERMS *(Continue on reverse if necessary and identify by block number)*
FIELD	GROUP	SUB-GROUP	Atmospheric Plasma; Broadband Absorption; Electron
20	09		Lifetime; Plasma Antenna.
17	04		

19. ABSTRACT *(Continue on reverse if necessary and identify by block number)*

Mean electron lifetimes and ionization techniques relevant to generating and sustaining a tenuous plasma in the Earth's atmosphere are presented. The mean electron lifetime, as a function of electron number density and altitude, was quantified by developing an air chemistry code. The code models deionization for initial conditions appropriate to single-pulse electron-beam or X-ray ionization of the atmosphere from sea level to 100,000 ft. The deionization model indicates that three-body attachment of electrons to oxygen is the dominate process for electron densities less that 10^{16} m^{-3}. For densities above 10^{18} m^{-3} two-body and three-body electron-ion recombination dominates and reduces the electron lifetime several orders of magnitude. An electron number density of $\sim 10^{18}$ m^{-3} is the highest number density that can be efficiently sustained without a severe reduction in electron lifetime. The electrical conductivity corresponding to 10^{18} electrons/m^3 in the atmosphere is ~ 5 mho-m^{-1}, i.e., the conductivity of seawater. It is suggested that a large plasma cloud could function as an electromagnetic absorber.

20. DISTRIBUTION/AVAILABILITY OF ABSTRACT ☐ UNCLASSIFIED/UNLIMITED ☒ SAME AS RPT. ☐ DTIC USERS	21 ABSTRACT SECURITY CLASSIFICATION UNCLASSIFIED	
22a. NAME OF RESPONSIBLE INDIVIDUAL Robert J. Barker	22b. TELEPHONE *(Include Area Code)* (202) 767·5011	22c. OFFICE SYMBOL NP

DD FORM 1473, 84 MAR
83 APR edition may be used until exhausted.
All other editions are obsolete.
SECURITY CLASSIFICATION OF THIS PAGE

ABSTRACT

Mean electron lifetimes and ionization techniques relevant to generating and sustaining a tenuous plasma in the Earth's atmosphere are presented. The mean electron lifetime, as a function of electron number density and altitude, was quantified by developing an air-chemistry code. The code models deionization for initial conditions appropriate to single-pulse electron-beam or X-ray ionization of the atmosphere from sea level to 100,000 ft. The deionization model indicates that three-body attachment of electrons to oxygen is the dominate process for electron densities less than 10^{16} m^{-3}. For densities above 10^{18} m^{-3} two-body and three-body electron-ion recombination dominates and reduces the electron lifetime several orders of magnitude. An electron number density of ~10^{18} m^{-3} is the highest number density that can be efficiently sustained without a severe reduction in electron lifetime. The electrical conductivity corresponding to 10^{18} electrons/m^3 in the atmosphere is ~ 5 mho-m^{-1}, i.e., the conductivity of seawater. It is suggested that a large plasma cloud could function as an electromagnetic absorber and that a long narrow plasma column could serve as a long wire antenna.

CONTENTS

FIGURES

TABLES

I INTRODUCTION

The Earth's lower atmosphere is a challenging environment in which to generate and maintain tenuous plasma clouds. The plasma clouds of interest have volumes from several hundred cubic meters to several thousand cubic meters. The electron number density of these tenuous plasma clouds varies from 10^{16} m^{-3} to 10^{20} m^{-3} and is low compared to the ambient atmospheric density of 10^{25} m^{-3} to 10^{23} m^{-3}. The challenge due to the Earth's atmosphere is to identify ionization techniques that maximize a cloud's lifetime while minimizing the energy required to sustain the plasma cloud.

The Earth's lower atmosphere consists of the troposphere, which extends from sea level to an altitutde of 10 km, and the stratosphere, which extends from 10 km to 45 km. The atmospheric number density is high enough that collisions between plasma electrons and neutral constituents in the atmosphere restrict electron motion. In general, cold collisionless plasma theory is sufficient to predict the electrical properties of these plasmas. The plasma deionization process that is dominated by prompt attachment of electrons to oxygen is more complex. A starting point to minimize the energy required to sustain a tenuous plasma cloud is to model the dominant attachment and detachment processes during a relevant time scale.

The difficulty in generating and maintaining a plasma is that the ionization process and subsequent deionization is a function of many parameters and numerous chemical reactions. These parameters include the variation (1) in atmospheric number density with altitude, (2) water vapor concentration, (3) electron number density, (4) source of ionization, and (5) concentration of ionization byproducts. Although a large number of parameters can be accomodated in a theoretical model and the dominant physical processes are known, exact modeling is not possible for three reasons.

First, the number of possible species and their excited states are too numerous to treat simultaneously. Second, some important air-chemistry reaction rates are poorly known and many have not been measured at all.

Many air-chemistry reaction rates relevant to electron-ion and ion-ion re-combination remain the subject of basic research. Third, there is a wide difference in time scales among the reactions relevant to recombination. Hence, the differential equations describing recombination process constitute a stiff system of differential equations.[1]* Therefore, the results of a modeling effort are not exact predictors of experiment, but broad indicators of what to expect.

To simplify the air-chemistry model, some characteristics of tenuous plasma clouds were postulated. The cloud should exist for 10 μs and have a volume of several thousand cubic meters. Clouds with those characteristics have applications such as an absorptive plasma cloud, a reflective plasma cloud, and as a plasma antenna. The 10-μs time scale substantially reduces the number of atmospheric species and the number of recombination reactions required by a computational model.

---

*References are listed at the end of this report.

II TECHNICAL APPROACH

An air-chemistry computational model was developed to characterize the ionization-recombination process in a tenuous collisional plasma. Basic assumptions in this model include a plasma volume between 10^2 m^3 and 10^4 m^3, an electron number density less than 10^{18} m^{-3}, and a plasma lifetime of 10 μs. These assumptions simplify the model and reduce its computational requirement so that a PC can manage them. This chapter contains a discussion of these assumptions and relevant parameters used in formulating the code.

A. AIR-CHEMISTRY ASSUMPTIONS

The air-chemistry code models the ionization-recombination process in a tenuous plasma cloud. Output from this code is useful in determining the energy required to generate and sustain the plasma. The plasma consists of the neutral atoms and molecules that naturally exist in the Earth's atmosphere plus electrons, ions, atoms, and molecules produced by an ionization source interacting with the atmosphere. Ionizing a large volume of air at atmospheric pressure for 10 μs implies (1) some distinguishing characteristics of the source of ionization, (2) some assumptions about the temperature of the plasma, and (3) the importance of diffusion. These implications result in three simplifications to the air-chemistry model.

The first simplification concerns the ionization source. Because uniform ionization of a large volume of air, tens of meters thick, is the goal, the ionization technique must be highly penetrating. Energetic X-rays and electron beams have sufficient range to produce substantial regions of ionization. In addition, these ionization sources produce plasma with a predictable electron number density with distance. The electron number density, $n_e(r)$, for these ionization sources is

$$n_e(r) = n_e(r_2)\left[\frac{r_2}{r}\right]^2 \exp\left[\frac{r_2 - r}{r_m}\right] \qquad , \qquad (2.1)$$

where r is the radial distance from a source, $n_e(r_2)$ is the electron number density at range r_2, and r_m is the 1/e range for X-ray or electron beam absorption.

The quantity $r_m = (n_m \sigma_m)^{-1}$ for X-ray ionization depends on the number density of the propagation medium (n_m) and the cross section for photoionization or photoabsorption (σ_m). Hudson and Kieffer [2] and Hubbel [3] have complied tables and curves of σ_m for most elements as a function of photon energy from 4 eV to 100 GeV. The Radiological Health Handbook [4] has curves of penetration distance versus energy from 10 keV to 10 MeV for several elements and substances that include air and water.

The quantity r_m for electron beam or beta ionization refers to the maximum range of the ionization. The Radiological Health Handbook has maximum range curves for electrons with energy from 100 keV to 4 MeV penetrating air and water. The computations of range evaluated with the continuously slowing down approximation by Pages et al [5] spans the energy range from 10 keV to 100 MeV and tabulates 59 elements, 55 compounds (including air), and soft tissue.

The second simplification is the equilibrium temperature of the tenuous plasma. It is possible to estimate this temperature for X-ray and beta-ray ionization sources. The total energy per unit volume to ionize air is $n_e E_i$, where E_i is the average energy to form an electron- ion pair. If all this energy results in atmospheric heating, then the temperature increase above the ambient temperature is

$$\Delta T = \frac{n_e E_i}{\rho c_v} \quad , \tag{2.2}$$

where ρ is the mass density of air and c_v ($= 1.00 \times 10^3 J/kg \, K$) is the specific heat of air. Tabulated values [6] of E_i are 41.5 eV for He, 34.6 eV for N_2, 31.8 eV for O_2, and 33.7 eV for air.

The temperature increase due to a single pulse of ionizing radiation at sea level for $n_e = 10^{18}$ m^{-3} is 4.09×10^{-3} K, 4.09×10^{-5} K for $n_e = 10^{16}$ m^{-3}, and 4.09×10^{-7} K for ne $= 10^{14}$ m^{-3}. At an altitude of 60,000 ft, the

pressure is one-tenth that at sea level, and the temperature increases ten times the values cited. The increase in ambient temperature produced by the energy deposited in a plasma cloud by a single ionizing pulse, or a thousand sequential ionizing pulses, is negligible. Consequently, the temperature of the plasma cloud is approximately the ambient temperature of the atmosphere.

The third simplification concerns the importance of diffusion. The ambipolar diffusion coefficient is

$$D_a = \frac{2k\ T_i}{m_i \nu_{iN}} \quad , \quad \quad (2.3)$$

where k ($= 1.38 \times 10^{-23}$ J/$^\circ$K) is Boltzmann's constant, T_i is the ion temperature, m_i is an ion mass (4.65×10^{-26} Kg for N_2^+), and ν_{iN} is the momentum transfer collision rate between ions and the neutral atmosphere. Because the anticipated heating of air is negligible, the ion temperature and ambient air temperature are effectively equal. The diffusion coefficient has a value of 2.5×10^{-5} m^2/s at sea level and increases to 2×10^{-3} m^2/s at 100,000 ft. The characteristic time for diffusion across a 1-m plasma slab ranges from 16,000 s at sea level to 200 s at 100,000 ft. Compared to the 10-μs time scale of interest, diffusion is a slow process.

In summary the principal assumptions for modeling plasma generation in the Earth's atmosphere are:

(1) Ionization via an X-ray or electron beam source.
(2) Plasma electrons rapidly thermalize to the ambient temperature of the atmosphere.
(3) Diffusion of plasma electrons is slow compared to the time scale of interest.

The next section contains atmospheric data and air-chemistry reactions to model the atmospheric deionization process.

B. ATMOSPHERIC PARAMETERS

Parameters relevant to plasma generation in the atmosphere include

(1) Air density and temperature as a function of altitude.

5

(2) Momentum transfer collision rate as a function of altitude.

(3) Dominant atomic and molecular species.

(4) Dominant deionization reaction and their reaction rates.

These parameters have been the subject of numerous investigations; relevant tabulations for them follow in this section.

The number density, temperature, and pressure as a function of altitude in Table 2.1 correspond to values of the U.S. standard atmosphere.[7] At altitudes of 10,000 ft and above, the ambient temperature is below the triple point for water, and the concentration of water vapor is negligible. From sea level to 10,000 ft, the concentration of water vapor is high enough to influence the evaluation of the electron- neutral momentum transfer collision rate.

Table 2.1

U.S. STANDARD ATMOSPHERE

Altitude		Pressure	Temperature		Number Density	Density
ft	m	(torr*)	K	C	Per m^3	kg/m^3
0	0	760	288	15	2.55×10^{25}	1.225
10,000	3,048	521	268	-5	1.88×10^{25}	0.903
20,000	6,096	348	248	-25	1.36×10^{25}	0.653
30,000	9,144	225	228	-45	9.54×10^{24}	0.458
40,000	12,190	141	216	-57	6.31×10^{24}	0.303
50,000	15,240	86.9	216	-57	3.89×10^{24}	0.187
60,000	18,290	54.3	216	-57	2.43×10^{24}	0.117
70,000	21,340	33.5	218	-55	1.48×10^{24}	0.071
80,000	24,380	21.3	221	-52	9.31×10^{23}	0.045
90,000	27,430	12.8	224	-49	5.52×10^{23}	0.027
100,000	30,480	7.96	227	-46	3.39×10^{23}	0.016

*1 torr - 133.3 NT/m^2

The momentum-transfer collision rate has two components: momentum transfer (1) to neutral atmospheric constituents and (2) to ions. The electron-neutral collision rate, ν_{eN} for a mixture is

$$\nu_{eN} = \sum_s n_s \nu_{es} \qquad , \qquad (2.4)$$

where the summation index, s, denotes N_2, O_2, or H_2O molecules, n_s is the molecular number density, and ν_{es} is the collision rate per molecule. Bortner and Bauer [8] have a table of collision rates for atmospheric molecules as a function of electron energy. The electron-neutral collision rate in Table 2.2 is a summation of the principal atmospheric constituents of the standard atmosphere as a function of altitude.

Table 2.2

ATMOSPHERIC MOMENTUM-TRANSFER COLLISION RATES

Altitude (ft)	Electron-Neutral[*] Collision Rate (s^{-1})	Electron-Ion Collision Rate Per Ion		
		$N_e = 10^{16} m^{-3}$ $m^3 s^{-1}$	$N_e = 10^{18} m^{-3}$ $m^3 s^{-1}$	$N_e = 10^{20} m^{-3}$ $m^3 s^{-1}$
0	4.70×10^{11}	4.69×10^{-9}	2.99×10^{-9}	1.30×10^{-9}
10,000	1.18×10^{11}	5.14	3.25	1.36
20,000	3.97×10^{10}	5.67	3.55	1.42
30,000	2.07×10^{10}	6.30	3.89	1.48
40,000	1.25×10^{10}	6.74	4.13	1.52
50,000	7.67×10^{9}	6.74	4.13	1.52
60,000	4.79×10^{9}	6.74	4.13	1.52
70,000	2.97×10^{9}	6.66	4.09	1.51
80,000	1.90×10^{9}	6.55	4.03	1.50
90,000	1.15×10^{9}	6.44	3.97	1.50
100,000	7.27×10^{8}	6.33	3.91	1.49

[*]N_2, O_2, and H_2O molecules and electrons in thermal equilibrium with the standard atmosphere with 50 percent relative humidity.

The electron-ion collision rate, ν_{ei}, has a useful formulation [9] as

$$\nu_{ei} = \frac{3.6 \times 10^{-6} \; N_i}{T_e^{3/2}} \; \ln\left[\frac{1.2 \times 10 \; T_e^{3/2}}{n_e^{1/2}} \right] \quad , \qquad (2.5)$$

where N_i is the number density of both positive and negative ions in m^{-3}, T_e is the electron temperature in K, and ν_{ei} has the units of s^{-1}. The electron-ion collision rate is important for plasmas with ion densities that exceed 10^{18} ions/m^3.

An atmospheric plasma consists of neutral constituents, primarily the permanent constituents of the atmosphere, plus products generated by an ionization source. The permanent constituents and their volume ratio in Table 2.3 apply to the U.S. standard atmosphere.[10] The concentrations for N_2O and NO are appropriate near the Earth's surface, the concentration for O_3 applies above 60,000 ft.

The neutral species, negative ions, and positive ions in Table 2.3 are appropriate for the ionization sources and chemical reactions currently included in the air-chemistry code. Additional excited states of atoms and molecules are known to exist and play a role in deionization. The restricted list of constituents reflects an effort to model the dominant processes and implement a deionization solution on an IBM AT computer.

The deionization air-chemistry reactions necessary to describe a tenuous plasma in the Earth's atmosphere for 10 μs must model

(1) Electron attachment to form negative ions.
(2) Charge-transfer reactions to form more stable ions.
(3) Neutral species reactions with atoms and excited state molecules formed as ionization byproducts.
(4) Two-body and three-body positive-ion electron recombination.
(5) Two-body positive-ion negative-ion recombination.
(6) Three-body cluster-ion recombination.

Appendix A tabulates the 143 reactions and reaction rates used in the air-chemistry code. As noted elsewhere, this air-chemistry code is not an exact predictor of phenomena, but rather, a broad indicator of experiments.

Table 2.3

COMPOSITION OF ATMOSPHERIC PLASMA

Composition of Atmosphere			
Permanent Constituent	Percent by Volume	Variable Constituent	Percent by Volume
N_2, NITROGEN	78.084	H_2O, WATER VAPOR	0 - 0.04
O_2, OXYGEN	20.948	O_3, OZONE	$0 - 12 \times 10^{-4}$
CO_2, CARBON DIOXIDE	0.033	NO, NITRIC OXIDE	$0 - 5 \times 10^{-8}$
He, HELIUM	5.24×10^{-4}		
CH_4, METHANE	1.5×10^{-4}		
N_2O, NITROUS OXIDE	0.27×10^{-4}		

Products of Ionization and Deionization

Neutral Species	
N, NITROGEN	NO, NITRIC OXIDE
O, OXYGEN	OH, HYDROXYL
$O(^1\Delta_g)$, SINGLET DELTA	H, HYDROGEN

Negative Ions		Positive Ions	
O^-		N_4^+	H_2O^+
O_2^-	$O_2^- \cdot H_2O$	N_2^+	$O_2^+ \cdot H_2O$
O_3^-		N^+	H_3O^+
O_4^-		O_4^+	$H_3O^+ \cdot OH$
CO_3^-	$CO_3^- \cdot H_2O$	O_2^+	$H_3O^+ \cdot H_2O$
CO_4^-	$CO_4^- \cdot H_2O$	O^+	He^+
		NO^+	He_2^+

The dominant neutral gases in the plasma are N_2, O_2, and CO_2 and have number densities many orders of magnitude greater than the electron/ion density. These dominant gases can serve as the third body in numerous reactions among electrons, negative ions, and positive ions. The speed of three-body reactions depends on the concentration of the third body. At sea level, many of the three-body reactions in Appendix A constitute the dominant reactions. At altitudes above 25,000 ft, these three-body reactions are slow compared to the two-body reactions often cited as the dominant reactions in the D layer, E layer, and F layer. The inclusion of three-body processes is an important distinction between lower atmospheric codes and ones intended for the upper atmosphere.

The concentration of water vapor below 25,000 ft is sufficient to open up additional reaction channels. Even though the concentration of H_2O is insufficient to be a dominant species, H_2O reacts readily to form positive and negative ions. These reactions generate the hydronium ion (H_3O^+), $O_2^+ \cdot H_2O$, and hydrated negative ions of O_2^-, CO_3^-, and CO_4^-. The reaction rates involving H_2O at sea level are fast, and the hydronium ion and hydrated negative ions dominate. Above 25,000 ft, the water-vapor concentration is insufficient to generate significant concentrations of hydronium and hydrated ions in 10 μs.

Free electrons in the plasma react three ways.

(1) Three-body recombination with a positive ion (where an electron is the third body).

(2) Two-body recombination with a positive ion.

(3) Attachment to oxygen via two-body and three-body processes.

At high electron densities, three-body recombination, which has a reaction rate propotional to the electron concentration squared, dominates. At moderate electron densities, two-body recombination, which has a rate constant proportional to the electron concentration becomes the dominate process. At a sufficiently low electron concentration, the three-body attachment of electrons to oxygen, for which oxygen is the third body, dominates. The section on results quantifies the range of electron concentrations over which each of these three processes becomes the dominant electron process.

10

After an ionization source generates electrons and positive ions, the formation of negative ions, and ion recombination progresses. The initial negative and positive ion species react with neutral constituents of the atmosphere to form more stable ion species. These new ion species consist of multiple-atom-charged molecules, referred to as cluster ions. Because cluster-ion formation is a three-body process, its rate of formation depends on altitude. The formation rate of cluster ions at sea level is faster than the two-body recombination of positive and negative ions. At high altitudes two-body recombination becomes an important process.

Appendix A contains several reactions involving helium, even though helium is a minor constituent of the atmosphere. Because maintaining an atmospheric plasma is an energy consuming process, a survey of gases was conducted to establish the least energy-consuming gas. Helium is energetically efficient to maintain because (1) it does not form negative ions and (2) it has the lowest two-body and three-body electron positive-ion recombination rate of the ion species surveyed.[11]

C. IONIZATION PARAMETERS

Because the 143 coupled reactions in Appendix A contain many important three-body reactions, the deionization solution is nonlinear. The time history for the concentration of any species, such as electrons, depends on its initial concentration and that of all the other ion species. This section quantifies (1) the ion production rate for electron beam/ X-ray ionization and (2) photodestruction as a means to photodetach electrons and to alter the negative ion populations.

1. ELECTRON-BEAM/X-RAY IONIZATION

Fast electrons or X-rays bombarding air produce essentially the same ions, neutral species, and excited state species. The principal ionizing process for electron-beam bombardment is impact ionization, $e + N_2 \rightarrow N_2^+ + e + e$. For an X-ray beam photoionization and Compton absorption are the ionizing process, $\phi + N_2 \rightarrow N_2^+ + e$. The ionization products for bombardment in air are independent of ionization source because the first ionizing event results in energetic secondary electrons. These secondary electrons have an

11

energy equal to the incident energy minus the energy for the first ionizing event. Ionization because of these secondary electrons and subsequent secondary electrons continuously degrades the electron energy below the ionization potential. This loss of energy is systematic and progresses in a statistical manner. Reference 12 contains a study of ionizing radiation bombarding air, Appendix B contains a complete listing of ionization products extracted from Reference 12 plus mass attenuation coefficients.

The ionization products used in the air-chemistry code are in Table 2.4. These products constitute a subset of the ionization products in Appendix B. The exclusion of most excited-state atoms and molecules was necessary to reduce the number of species and the number of reactions required by the air-chemistry code. To compensate for the omitted excited-state species, which required ~5 eV of the 33.7 eV per electron-ion pair to generate, these excited-state species were included as ground-state species.

Table 2.4

ELECTRON BEAM/X-RAY IONIZATION PRODUCTS

Species	Particles Per Electron-Ion Pair
N_2^+	0.64
N^+	0.14
N	1.01
O_2^+	0.17
O^+	0.07
O^-	0.02
O	0.33
$O(^1\Delta_g)$	0.78

12

This approximation biases subsequent predictions of free-electron life-
time to slightly shorter values because two electron-detachment mechanisms
are omitted. In the first mechanism, excited-state species can detach elec-
trons directly for O_2^- in two-body collisions. In the second mechanism
excited-state species could interact with O_2 and excite a vibrational state.
Subsequent collisions of O_2^* with O_2^- favor electron detachment.

2. PHOTODESTRUCTION

The properties of negative ions in Table 2.5 [8] indicates that the elec-
tron attachment energy and molecular dissociation energies are of the order
of a few electron volts and vibrational energies are of the order of 0.1 eV.
Because these energies are small compared to the 33.7 eV necessary to gener-
ate an electron-ion pair, several techniques to detach electrons from nega-
tive ions were investigated. One investigation found that the internal ener-
gy of a negative ion that exists in an excited state effectively reduces the
amount of energy necessary for electron detachment. This excited-state ion
can be thought of as a ground-state ion elevated to a higher temperature.

For example, consider the collisional detachment of an electron,
$O_2^- + N_2 \rightarrow O_2 + N_2 + e$ (A25). The reaction rate for ground state O_2^- at 288 K
is 5×10^{-20} cm^3/s. If the O_2^- molecule is in its first vibrational level
$O_2^-(\nu - 1)$ at 0.132 eV, it has an effective temperature of 1500 K. The reac-
tion rate at 1500 K is 7×10^{-13} cm^3/s--over seven orders of magnitude
larger. At an altitude of 30,000 ft, the density of nitrogen is 7×10^{18}
cm^{-3}, and the time constant for electron detachment from ground state O_2^- is
2.8 s, but 200 ns from $O_2^-(\nu - 1)$. Consequently, excitation of O_2^- from its
ground state to excited state transforms a benign detachment mechanism into
a dominate process.

Although the rapid detachment rates of excited state negative ions are
easy to predict, techniques to form them in the atmosphere are not as easy.
Because the species O^- and O_2^- do not have dipole moments, single photon
transitions to an excited state are forbidden transitions. Multiphoton and
collisional excitation is, however, possible. A continuum light source
operating above the electron attachment/dissociation energy can photodetach
electrons and dissociate cluster ions into O^- and O_2^-. Some of the

13

dissociation products will be in the ground state, but some will exist in
an excited state and subsequently detach in collisions with N_2.

<div align="center">

Table 2.5

NEGATIVE-ION PROPERTIES

</div>

Property	Negative Ions						
	O^-	O_2^-	O_3^-	O_4^-	CO_3^-	CO_4^-	$O_2 \cdot H_2O^-$
Electron Affinity (eV)	1.47	0.43	1.9	1.0	——	1.2	1.2
Vertical Detachment Energy (eV)	1.47	0.5	2.1	1.0	-——	1.2	1.2
Dissociation Energy (eV) (Dissociation Products)	—	4.06 $(O^-, 0)$	1.4 (O^-, O_2) 2.5 (O_2^-, O)	0.54 (O_2^-, O_2)	—— (O^-, CO^2)	0.8 (O_2^-, CO_2)	0.8 (O_2^-, H_2O)
Vibrational Level (cm^{-1}) [eV]	— — —	1065 [0.132] —— ——	1260 [0.156] 800 [0.099] 1140 [0.141]	—— —— ——	—— —— ——	—— —— ——	—— —— ——

Photon absorption in the atmosphere and the cross sections for photo-
destruction in Table 2.6 [13] define the wavelength characteristics of the
continuum source. The Schuman-Runge continuum and bands caused by oxygen
strongly absorb photons with wavelengths less than 200 nm (6.88 eV). And
the cross sections for photodestruction of cluster ions are of the order of
10 MB (1 MB = 10^{-18} cm^2) at 250 nm, but decrease to 1 MB at 620 nm (2.0 eV).
Hence, the continuum source is an ultraviolet (UV) source operating between

620 nm and 200 nm. Commercial UV flash lamps, manufactured by the XENON
Corporation, operate at 30% efficiency with an emission spectrum from 200 nm
to 1000 nm.

Table 2.6

NEGATIVE-MOLECULE PHOTODESTRUCTION CROSS SECTIONS

Wavelength Energy	Cross Sections For Negative Ions in MB (10^{-18} cm^2)						
	O^-	O_2^-	O_3^-	O_4^-	CO_3^-	CO_4^-	$O_2 \cdot H_2O^-$
248.4 nm (4.99 eV)	11.3	9.5	10.2	13.1	2.7	10.1	8.5
351.1 nm (3.53 eV)	8.2	3.4	2.3	8.4	——	——	——
350.7 nm (3.53 eV) and 356.4 nm (3.47 eV)	8.2	3.7	2.1	8.6	0.07	0.45	2.6
406.7 nm (3.05 eV)	6.3	2.6	5.0	2.9	0.4	——	1.6
413.1 nm (3.00 eV)	6.3	2.6	3.7	3.2	0.4	<0.06	1.5
620.0 nm (2.00 eV)	6.3	1.3	0.09	1.1	1.5	<0.02	0.3

The utilization of an UV flash lamp is an attractive technique to detach
electrons, dissociate cluster ions, and generate excited-state ions in an
optically thick plasma. Consider an atmospheric plasma 20-m thick; it is
optically thick for a cluster-ion density of ~10^{20} m^{-3} (10^{14} ions/cm^3).
This photodestruction technique would work in conjunction with other ioni-
zation sources to maintain a plasma. A plasma with an electron density of
10^{16} m^{-3} could, for example, be generated and sustained by repeated electron-
beam/X-ray ionization until the negative-ion density built up to 10^{20} m^{-3}.
UV illumination of this plasma could then help to sustain this plasma.

The investigation of the UV ionization technique is not complete and is the subject of investigation in the next funding period. The feasibility of this technique depends on the excited-states generated, the electron density, and the duration of the plasma.

D. COMPUTER IMPLEMENTATION

A code was written on an IBM AT computer to model the deionization of air. The atmospheric and ionization parameters discussed in Sections II.B. and II.C were coded into data arrays within subroutines. This provided initial conditions for the electron concentration plus the 37 atmospheric species in Table 2.3 as a function of altitude.

The system of nonlinear differential equations to model deionization is

$$\frac{dy_i}{dt} = f_i(t, y_1, y_2, \ldots, y_{38}) \qquad i = 1, 38 \qquad (2.6)$$

$$f_i = y_i \sum_{j=1}^{38} n_{ij} \, k_{ij} \, y_j + y_i \sum_{m=1}^{38} \sum_{j=1}^{38} n_{ijm} \, y_j \, y_m \qquad (2.7)$$

where y_i denotes the $i\underline{th}$ species and f_i is a function involving the rate constants in Appendix A for reactions among the $i\underline{th}$, $j\underline{th}$, and $m\underline{th}$ species. The terms k_{ij} and k_{ijm} refer to two-body and three-body reaction rates, respectively. The term n_{ij} or n_{ijm} is the integer number of the $i\underline{th}$ species produced or consumed per reaction. The term n_{ij} or n_{ijm} is positive if the $i\underline{th}$ species is produced, and negative if it is consumed.

Although there are 38 simultaneous equations in the deionization solution, Euler's method proved to be a satisfactory technique for a time scale of 10 μs. The solution begins with a time step of 5×10^{-12} s and increases slowly up to a time of 1 ns. Thereafter, the time is in 1-ns increments. At the end of each increment, charge conservation is imposed with any imbalance absorbed by the positive ion species. Computing the deionization solution beyond 10 μs with Euler's method is prone to error because the system

16

of equations becomes too stiff. The more sophisticated solution techniques to be implemented during the second funding period are necessary to extend the deionization solution beyond 10 μs.

E. PLASMA CONDUCTIVITY AND APPLICATIONS

A man-made collisional atmospheric plasma has controlable electromagnetic properties. The plasma properties are controlable because the electron density is a controlable quantity. The electron density depends on the amount of energy dissipated to generate the plasma and the power applied to sustain the plasma thereafter. The dispersion relation and ac conductivity of an atmospheric plasma succintly define the properties of plane-wave propagation through a plasma cloud. These properties suggest straightforward applications.

The dispersion relation expressed in terms of the ac conductivity, $\sigma(\omega)$, for a cold collisional plasma is

$$k(\omega) - \frac{\omega}{c} \left[1 - \frac{i\sigma(\omega)}{\omega \epsilon_o} \right]^{1/2} \tag{2.8}$$

$$\sigma(\omega) - \frac{n_e e^2}{m_e(\nu + i\omega)} + \sum \frac{n_i e^2}{m_i(\nu_{iN} + i\omega)} \tag{2.9}$$

where k is the wave number and ω (= $2\pi f$) is the angular frequency. The term m_e is the electron mass, c is the speed of light, and ϵ_o is the permittivity constant in MKS units. The collision rate for electrons, $\nu - \nu_{eN} + \nu_{ei}$, is the sum of the electron-neutral and electron-ion momentum transfer collision rates. The summation for ion conductivity in Eq. (2.9) is generally small compared to the electron conductivity. The ion contribution is important because ions persist much longer than electrons in the atmosphere. For a plasma sustained by repeated ionization, the ion density may become the principal contributor to the conductivity in Eq. (2.9).

The electrical properties in Table 2.7 typify an atmospheric plasma at 40,000 ft. For an electron number density less than 10^{13} m^{-3}, the

17

conductivity is less than 2.8×10^{-5} mho-m^{-1} and approximates a free-space condition. The real part of the wave number (k_r) is essentially that of free space. Attenuation, predicted from the imaginary part of the wave number (k_i), is inconsequential across a 20-m plasma cloud.

Table 2.7

ELECTRICAL PROPERTIES

Electron Density m^{-3}	Plasma Frequency f_p	dc Electron Conductivity (mho-m^{-1})	Wave Number, m^{-1}		Attenuation per Meter (dB)
			k_r	k_i	
10^{10}	899.0 KHz	2.8×10^{-8}	21.00	-3.8×10^{-6}	-0.0
10^{11}	2.84 MHz	2.8×10^{-7}	21.00	-3.8×10^{-5}	-0.0
10^{12}	8.99 MHz	2.8×10^{-6}	21.00	-3.8×10^{-4}	-0.0
10^{13}	28.4 MHz	2.8×10^{-5}	21.00	-3.8×10^{-3}	-0.0
10^{14}	89.9 MHz	2.8×10^{-4}	20.98	-3.8×10^{-2}	-0.3
10^{15}	284.0 MHz	2.8×10^{-3}	20.77	-3.8×10^{-1}	-3.3
10^{16}	899.0 MHz	2.8×10^{-2}	18.93	-4.2	-36.5
10^{17}	2.84 GHz	2.8×10^{-1}	23.60	-3.4×10^{1}	-295.0
10^{18}	8.99 GHz	2.8	67.28	-1.2×10^{2}	-1,042.0
10^{19}	28.4 GHz	2.8×10^{1}	210.5	-3.8×10^{2}	-3,300.0
10^{20}	89.9 GHz	2.8×10^{2}	665.0	-1.2×10^{3}	-10,423.0

DATA: Altitude of 40,000 ft., $\nu = 10^{10}$ s^{-1}, f = 1 GHz

For electron number densities between 10^{14} m^{-3} and 10^{18} m^{-3}, the conductivity of an atmospheric plasma increases from that of fresh water, 10^{-4} mho-m^{-1}, to that of sea water, 5 mho-m^{-1}. Electromagnetic absorption is significant: -3 dB/m for $n_e = 10^{15}$ m^{-3} and -36.5 dB/m for $n_e = 10^{16}$ m^{-3}. Higher electron densities continue to increase conductivity and absorption.

In addition to absorption, a wave can reflect from a plasma cloud. At an electron density, for which the plane-wave frequency (f) equals the

18

plasma frequency, $f_p = [n_e e^2/(4\pi^2 \epsilon_0 m_e)]^{1/2}$, k_r deviates from its free-space value. For $n_e = 10^{18}$ m^{-3}, k_r is three times its free space value and implies the medium has an index of refraction of three. Traditional Fresnel reflection theory dictates that a wave will reflect from a slab-like discontinuity. But the ionization sources suggested in Section II.A have $1/r^2$ electron-density variations. The reflection coefficient is less than the Fresnel reflection coefficient because the index of refraction varies slowly and continuously over a distance of one wavelength.

Consider a wave propagating into a plasma cloud towards an ionization source. The sequence for reflection is absorption into the cloud, reflection from a region with $f_p > f$, and absorption out of the cloud. The round-trip absorption can be significant. This absorption is also broadband because the ac conductivity does not appreciably deviate from the dc conductivity in Table 2.7 for $f \leq \nu/2\pi$.

An electron beam operating in conjunction with a focused UV flash lamp could generate a plasma column. The column illuminated by the flash lamp could be used as a plasma antenna. Repeated operation of the UV flash lamp sustains the plasma antenna via the method suggested in Section C.2. At a frequency of 150 MHz and $n_e = 10^{18}$ m^{-3}, the conductivity is 2.8 mho-m^{-1}, and the skin depth is 4 cm. A plasma column 8 cm in diameter 20-m long could form a plasma antenna.[14] This antenna would have a resistance of 71 ohms/m and be useful for intermittent HF and VHF communications.

An atmospheric plasma with n_e above 10^{18} m^{-3} has a conductivity in the range of a semiconductor. Although the absorption of electromagnetic waves in intense and the reflection coefficient high, electron recombination processes are rapid. Applications are the same as for lower density plasmas, but require additional power, for reasons explained in the next section.

19

III RESULTS

The major results during the first year consisted of (1) implementing an air-chemistry code, (2) establishing UV photodestruction as a promising ionization technique, (3) identifying helium as an efficient gas, and (4) determining free-electron lifetime as a function of altitude and electron density. The air-chemistry code and UV photodestruction have been discussed in Chapter II, but the helium gas and electron lifetime studies require further explanation.

As a result of many discussions with SRI and the personnel at Wright-Patterson Air Force Base about atmospheric plasmas, the question, what is the most energy efficient gas to ionize and maintain at sea level pressures, continually arose. Noble gases were identified because they do not readily form negative ions. Hence, electron attachment processes do not deplete the electron density: electron positive-ion recombination does. Helium has the advantage of the lowest recombination coefficients for both He^+ and its dimmer, He_2^+. [11] Helium was included in the air-chemistry code with air acting as an impurity. Data from running the air-chemistry code indicates that air concentrations below 1 ppm do not seriously affect the electron-ion recombination time in helium at atmospheric pressure. The recombination time is ~1 ms, five orders of magnitude larger than air!

The invention disclosure, "Broadband Electromagnetic Absorption Via a Collisional Helium Plasma," included here as Appendix C, was filed during May 1986.

Figure 3.1 succinctly reports the electron lifetime study computed with the air-chemistry code. The electron lifetime refers to the time required for the electron density to decrease by a factor of e^{-1}. These lifetimes are appropriate for a plasma generated by an electron beam or X-ray source in ambient air. The most efficient plasma generation occurs for $n_e \leq 10^{16}$ m^{-3}, in which three-body attachment of electrons to oxygen dominates. The electron lifetime diminishes rapidly for $n_e > 10^{18}$ m^{-3} as electron positive-ion recombination becomes more important.
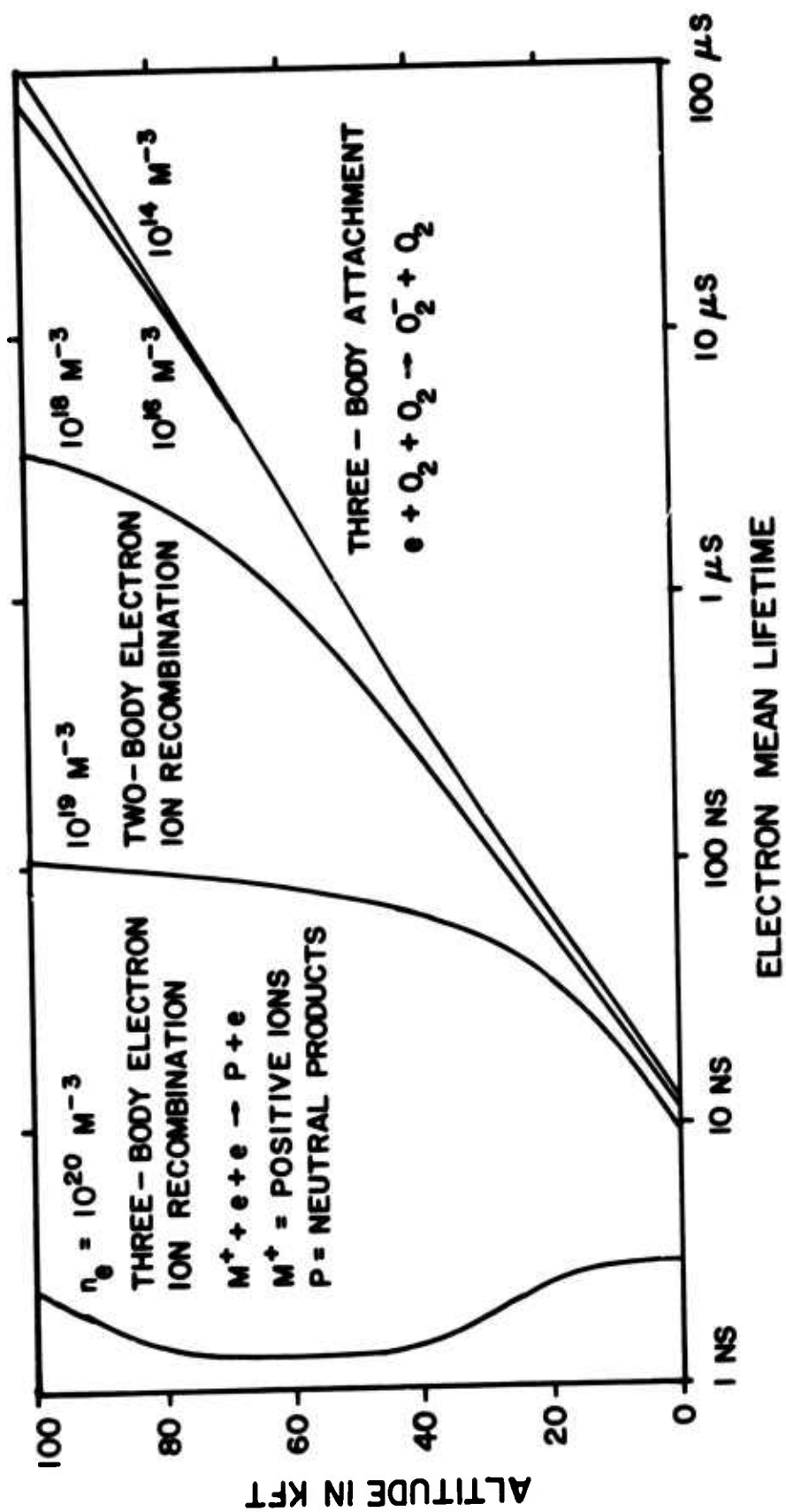
FIGURE 3.1 ELECTRON LIFETIME IN THE ATMOSPHERE

21

Electron heating or ion heating can increase the electron lifetime by lowering the two-body and three-body reaction rates. But those heating techniques require a considerable expenditure of energy, because momentum transfer from charged species to the neutral atmosphere is fast compared to 10 μs. Charged specie heating techniques, therefore, effectively increase the ambient air temperature.

The important fact to note is that the electron lifetime for $n_e < 10^{18}$ m^{-3} is limited by electron attachment to oxygen. A density of $n_e - 10^{16}$ m^{-3} could, for example, be sustained by repetitively ionizing the same volume of air. At least 100 sequential ionization events could occur before the positive-ion species would have sufficient density to alter the mean electron lifetime. Consequently, electron densities of ~10^{16} m^{-3} can be sustained for approximately 10 μs at altitudes above 25,000 ft.

The photodestruction technique requires a negative-ion density of ~10^{20} m^{-3} to be optically thick. Because two-body and three-body electron positive-ion recombination will shorten the electron lifetime, the ionization volume must be minimized to reduce the overall expenditure of energy. Because a UV flashlamp can be focused into a beam, it caters to defining a long narrow column of plasma. A plasma volume with n_e ~10^{18} m^{-3} could serve as a plasma antenna. Increasing n_e above 10^{18} m^{-3} would be energetically expensive because of the corresponding higher positive-ion concentration.

In summary, upper limits on the electron number density for man-made atmospheric plasma clouds have been computed. Large plasma clouds with n_e ~ 10^{16} m^{-3} can be sustained for 10 μs via repeated ionization at altitudes above 25,000 ft. And a low volume plasma column can have a density of n_e ~ 10^{18} m^{-3} for longer periods. The electrical conductivity for $n_e - 10^{16}$ m^{-3} approximates the conductivity of a good soil (~10^{-2} mho-m^{-1}) and implies significant broadband electromagnetic attenuation. A narrow plasma column with $n_e - 10^{18}$ m^{-3} has a conductivity comparable to seawater (5 mho-m^{-1}) and could serve as a long wire antenna at HF and VHF.

IV PERSONNEL, INTERACTIONS, AND PUBLICATIONS

The professional personnel associated with this research effort have
been:

> Don Eckstrom, Program Manager, Molecular Physics
>
> Gwen George, Research Analyst
>
> Tom Hedges, Program Director, Remote Measurements Laboratory
>
> Paul Titterton, Research Physicist
>
> Robert Vidmar, Principal Investigator, Senior Research Physicist

A preliminary draft of a manuscript entitled "Atmospheric Plasmas with
Applications to Electromagnetics" was prepared for later submission to IEEE
Antennas and Propagation. It is not complete and was not submitted, because
the air-chemistry code must be thoroughly validated against experimental
data. Only partial validation was possible with the Euler's method air-
chemistry solution implemented during the first year. During the second
year of funding, a stiff differential equation solver will be implemented
and complete validation will be possible.

Although no papers were presented, the principal investigator attended
a Gaseous Electronics Conference and an American Physical Society meeting.
Personal contacts with individuals from several institutions resulted and
atmospheric plasmas, ionization techniques, and deionization code implementa-
tion were topics of discussions. The concept of atmospheric plasma clouds
and electromagnetic applications were formally presented to Dr. David
Berrie, Dr. Brian Kent, and Mr. Joseph Faison of AFWAL/CDJ on 7 May 1986.

The interaction with AFWAL/CDJ resulted in a subsequent investigation
of helium plasma and the invention disclosure in Appendix C.

Appendix A

ATMOSPHERIC REACTION RATES

Appendix A

ATMOSPHERIC REACTION RATES

The reactions and reaction rates in this Appendix were extracted from Bortner and Bauer.[*] They are organized into five sections: negative-ion reactions; positive-ion reactions; neutral-specie reactions; positive-ion electron recombination; two-body positive-ion negative-ion recombination, and three-body cluster-ion recombination.

A. NEGATIVE-ION REACTIONS

Reaction	Rate
A1. $e + O_2 \rightarrow O^- + O$	$1.0E(-16)$ cm^3/s
A2. $e + O_3 \rightarrow O^- + O_2$	$9.0E(-12)$ cm^3/s
A3. $e + O_2 + O_2 \rightarrow O_2^- + O_2$	$1.4E(-29)\left(\dfrac{300}{T_e}\right) \exp\left(\dfrac{-600}{T_e}\right)$ cm^6/s
A4. $e + O_2 + N_2 \rightarrow O_2^- + N_2$	$1.0E(-31)$ cm^6/s
A5. $e + O_2 + H_2O \rightarrow O_2^- + H_2O$	$1.4E(-29)$ cm^6/s
A6. $e + O_2 + CO_2 \rightarrow O_2^- + CO_2$	$3.3E(-30)$ cm^6/s
A7. $e + O_2 + He \rightarrow O_2^- + He$	$1.0E(-31)$ cm^6/s
A8. $O^- + O \rightarrow O_2 + e$	$2.0E(-10)$ cm^3/s
A9. $O^- + N \rightarrow NO + e$	$2.0E(-10)$ cm^3/s
A10. $O^- + O_2 \rightarrow O_3 + e$	$5.0E(-15)$ cm^3/s
A11. $O^- + O_2(^1\Delta_g) \rightarrow O_3 + e$	$3.0E(-10)$ cm^3/s
A12. $O^- + O_2(^1\Delta_g) \rightarrow O_2^- + O$	$1.0E(-10)$ cm^3/s

---

[*]M. H. Bortner and T. Bauer, <u>Defense Nuclear Agency Reaction Rate Handbook</u>, 2nd Ed. (DASAIC, Santa Barbara, CA, 1972).

A13. $O^- + O_3 \rightarrow O_3^- + O$ $5.3E(-10)$ cm^3/s

A14. $O^- + N_2 \rightarrow N_2O + e$ $1.0E(-14)$ cm^3/s

A15. $O^- + NO \rightarrow NO_2 + e$ $2.5E(-10)\left(\dfrac{300}{T_{air}}\right)^{0.8}$ cm^3/s

A16. $O^- + O_2 + O_2 \rightarrow O_3^- + O_2$ $1.0E(-30)$ cm^6/s

A17. $O^- + O_2 + CO_2 \rightarrow CO_3^- + O_2$ $3.1E(-28)\left(\dfrac{300}{T_{air}}\right)$ cm^6/s

A18. $O^- + O_2 + He \rightarrow O_3^- + He$ $1.0E(-30)$ cm^6/s

A19. $O_2^- + O \rightarrow O^- + O_2$ $1.5E(-10)$ cm^3/s

A20. $O_2^- + N \rightarrow NO_2 + e$ $3.0E(-10)$ cm^3/s

A21. $O_2^- + N \rightarrow O^- + NO$ $1.0E(-10)$ cm^3/s

A22. $O_2^- + O_2 \rightarrow O_2 + O_2 + e$ $2.7E(-10)\left(\dfrac{T_{O_2^-}}{300}\right)^{\frac{1}{2}} \exp\left(\dfrac{-5590}{T_{O_2^-}}\right)$ cm^3/s

A23. $O_2^- + O_2(^1\Delta_g) \rightarrow O_2 + O_2 + e$ $2.0E(-10)$ cm^3/s

A24. $O_2^- + O_3 \rightarrow O_2 + O_3^-$ $4.0E(-10)$ cm^3/s

A25. $O_2^- + N_2 \rightarrow O_2 + N_2 + e$ $1.9E(-12)\left(\dfrac{T_{O_2^-}}{300}\right)^{1.5} \exp\left(\dfrac{-4990}{T_{O_2^-}}\right)$ cm^3/s

A26. $O_2^- + O_2 + O_2 \rightarrow O_4^- + O_2$ $3.5E(-31)\left(\dfrac{300}{T_{air}}\right)$ cm^6/s

A27. $O_2^- + O_2 + H_2O \rightarrow O_2^- \cdot H_2O + O_2$ $3.0E(-28)\left(\dfrac{300}{T_{air}}\right)$ cm^6/s

A28. $O_2^- + O_2 + CO_2 \rightarrow CO_4^- + O_2$ $4.7E(-29)\left(\dfrac{300}{T_{air}}\right)$ cm^6/s

A29. $O_2^- + O_2 + He \rightarrow O_4^- + He$ $3.5E(-31)\left(\dfrac{300}{T_{air}}\right)$ cm^6/s

A30. $O_3^- + O \rightarrow O_2 + O_2 + e$ $1.0E(-11)$ cm^3/s

A31. $O_3^- + O \rightarrow O_2^- + O_2$ $3.2E(-10)$ cm^3/s

A32. $O_3^- + CO_2 \rightarrow CO_3^- + O_2$ $5.5E(-10)\left(\dfrac{300}{T_{air}}\right)^{0.49}$ cm^3/s

A33. $O_4^- + O \rightarrow O_3^- + O_2$ $4.0E(-10)$ cm^3/s

A34. $O_4^- + O_2 \rightarrow O_2^- + O_2 + O_2$ $2.7E(-14)$ cm^3/s

A35. $O_4^- + O_3 \rightarrow O_3^- + O_2 + O_2$ $3.0E(-10)$ cm^3/s

A36. $O_4^- + CO_2 \rightarrow CO_4^- + O_2$ $4.3E(-10)$ cm^3/s

A37. $O_4^- + H_2O \rightarrow O_2^- \cdot H_2O + O_2$ $1.4E(-9)$ cm^3/s

A38. $O_2^- \cdot H_2O + O_3 \rightarrow O_3^- + O_2 + H_2O$ $2.3E(-10)$ cm^3/s

A39. $O_2^- \cdot H_2O + CO_2 \rightarrow CO_4^- + H_2O$ $5.8E(-10)$ cm^3/s

A40. $CO_3^- + O \rightarrow O_2^- + CO_2$ $1.1E(-10)$ cm^3/s

A41. $CO_3^- + O_2 + H_2O \rightarrow CO_3^- \cdot H_2O + O_2$ $1.0E(-28)\left(\dfrac{300}{T_{air}}\right)$ cm^6/s

A42. $CO_4^- + O \rightarrow CO_3^- + O_2$ $1.5E(-10)$ cm^3/s

A43. $CO_4^- + O_2 \rightarrow O_4^- + CO_2$ $2.0E(-14)$ cm^3/s

A44. $CO_4^- + O_3 \rightarrow O_3^- + CO_2 + O_2$ $1.3E(-10)$ cm^3/s

A45. $CO_4^- + N_2 + H_2O \rightarrow CO_4^- \cdot H_2O + N_2$ $5.0E(-29)\left(\dfrac{300}{T_{air}}\right)$ cm^6/s

B. POSITIVE-ION REACTIONS

Reaction	Rate
B1. $N^+ + O_2 \rightarrow N + O_2^+$	$3.0E(-10)$ cm^3/s
B2. $N^+ + O_2 \rightarrow NO^+ + O$	$2.8E(-10)$ cm^3/s
B3. $N^+ + H_2O \rightarrow H_2O^+ + N$	$2.6E(-9)$ cm^3/s
B4. $N_2^+ + O \rightarrow NO^+ + N$	$1.3E(-10)\left(\dfrac{300}{T_{air}}\right)^{0.46}$ cm^3/s
B5. $N_2^+ + N_2 + N_2 \rightarrow N_4^+ + N_2$	$5.0E(-29)$ cm^6/s

B6. $N_2^+ + N_2 + He \rightarrow N_4^+ + He$ $\qquad$ $5.0E(-29)$ cm^6/s

B7. $N_4^+ + O_2 \rightarrow O_2^+ + N_2 + N_2$ $\qquad$ $4.0E(-10)$ cm^3/s

B8. $O^+ + O_2 \rightarrow O_2^+ + O$ $\qquad$ $2.0E(-11)\left(\dfrac{300}{T_{air}}\right)^{0.4}$ cm^3/s

B9. $O^+ + H_2O \rightarrow H_2O^+ + O$ $\qquad$ $2.33E(-9)$ cm^3/s

B10. $O^+ + N_2 + N_2 \rightarrow NO^+ + N + N_2$ $\qquad$ $6.0E(-29)\left(\dfrac{300}{T_{air}}\right)^{2}$ cm^6/s

B11. $O_2^+ + N \rightarrow NO^+ + O$ $\qquad$ $1.2E(-10)$ cm^3/s

B12. $O_2^+ + O_2 + O_2 \rightarrow O_4^+ + O_2$ $\qquad$ $2.8E(-30)$ cm^6/s

B13. $O_2^+ + O_2 + He \rightarrow O_4^+ + He$ $\qquad$ $2.8E(-30)$ cm^6/s

B14. $O_2^+ + H_2O + N_2 \rightarrow O_2^+ \cdot H_2O + N_2$ $\qquad$ $2.8E(-28)\left(\dfrac{300}{T_{air}}\right)^{2}$ cm^6/s

B15. $O_4^+ + O \rightarrow O_2^+ + O_3$ $\qquad$ $3.0E(-10)$ cm^3/s

B16. $O_4^+ + O_2(^1\Delta_g) \rightarrow O_2^+ + O_2 + O_2$ $\qquad$ $1.0E(-10)$ cm^3/s

B17. $O_4^+ + N_2 \rightarrow O_2^+ + O_2 + N_2$ $\qquad$ $2.6E(-5)\left(\dfrac{300}{T_{air}}\right)^{4.2}\exp\left(\dfrac{-5400}{T_{air}}\right)$ cm^3/s

B18. $O_4^+ + H_2O \rightarrow O_2^+ \cdot H_2O + O_2$ $\qquad$ $1.5E(-9)$ cm^3/s

B19. $He^+ + N_2 \rightarrow N^+ + N + He$ $\qquad$ $6.0E(-10)$ cm^3/s

B20. $He^+ + N_2 \rightarrow N_2^+ + He$ $\qquad$ $6.0E(-10)$ cm^3/s

B21. $He^+ + O_2 \rightarrow O^+ + O + He$ $\qquad$ $6.0E(-10)$ cm^3/s

B22. $He^+ + O_2 \rightarrow O_2^+ + He$ $\qquad$ $6.0E(-10)$ cm^3/s

B23. $He^+ + He + He \rightarrow He_2^+ + He$ $\qquad$ $1.1E(-31)$ cm^6/s

B24. $He_2^+ + N_2 \rightarrow N_2^+ + He + He$ $\qquad$ $1.2E(-9)$ cm^3/s

B25. $O_2^+ \cdot H_2O + O_2 \rightarrow O_4^+ + H_2O$ $\qquad$ $9.4E(-14)$ cm^3/s

B26. $O_2^+ \cdot H_2O + O_2(^1\Delta_g) \rightarrow O_4^+ + H_2O + O_2$ $\qquad$ $1.0E(-10)$ cm^3/s

B27. $O_2^+ \cdot H_2O + NO \rightarrow NO^+ + H_2O + O_2$ $\qquad$ $1.0E(-10)$ cm^3/s

B28. $O_2^+ \cdot H_2O + H_2O \rightarrow H_3O^+ \cdot OH + O_2$ 1.0E(-9) cm^3/s

B29. $H_2O^+ + O_2 \rightarrow O_2^+ + H_2O$ 2.0E(-10) cm^3/s

B30. $H_2O^+ + H_2O \rightarrow H_3O^+ + OH$ 1.8E(-9) cm^3/s

B31. $H_3O^+ + H_2O + N_2 \rightarrow H_3O^+ \cdot H_2O + N_2$ 3.4E(-27) cm^6/s

B32. $H_3O^+ \cdot OH + H_2O \rightarrow H_3O^+ \cdot H_2O + OH$ 1.0E(-9) cm^3/s

C. NEUTRAL-SPECIE REACTIONS

Reaction	Rate
C1. $N + N + N_2 \rightarrow N_2 + N_2$	7.6E(-34) $\exp\left(\dfrac{500}{T_{air}}\right)$ cm^6/s
C2. $O + O + N_2 \rightarrow O_2 + N_2$	3.0E(-33) $\left(\dfrac{300}{T_{air}}\right)^{2.9}$ cm^6/s
C3. $O + O_2 + N_2 \rightarrow O_3 + N_2$	5.5E(-34) $\left(\dfrac{300}{T_{air}}\right)^{2.6}$ cm^6/s
C4. $O_2(^1\Delta_g) + O_2 \rightarrow O_2 + O_2$	2.4E(-18) cm^3/s
C5. $O_2(^1\Delta_g) + N_2 \rightarrow O_2 + N_2$	1.1E(-19) cm^3/s
C6. $O_2(^1\Delta_g) + H_2O \rightarrow O_2 + H_2O$	1.5E(-17) cm^3/s

D. POSITIVE-ION ELECTRON RECOMBINATION

Reaction	Rate
D1. $N^+ + e + e \rightarrow N + e$	7.0E(-20) $\left(\dfrac{300}{T_e}\right)^{4.5}$ cm^6/s
D2. $N^+ + e + N_2 \rightarrow N + N_2$	6.0E(-27) $\left(\dfrac{300}{T_e}\right)^{2.5}$ cm^6/s
D3. $N_2^+ + e + e \rightarrow N_2 + e$	7.0E(-20) $\left(\dfrac{300}{T_e}\right)^{4.5}$ cm^6/s
D4. $N_2^+ + e \rightarrow N + N$	2.7E(-7) $\left(\dfrac{300}{T_e}\right)^{0.2}$ cm^3/s

D5. $N_4^+ + e \rightarrow N_2 + N_2$ $2.0E(-6)\ cm^3/s$

D6. $O^+ + e + e \rightarrow O + e$ $7.0E(-20)\left(\dfrac{300}{T_e}\right)^{4.5}\ cm^6/s$

D7. $O^+ + e + O_2 \rightarrow O + O_2$ $6.0E(-27)\left(\dfrac{300}{T_e}\right)^{2.5}\ cm^6/s$

D8. $O_2^+ + e + e \rightarrow O_2 + e$ $7.0E(-20)\left(\dfrac{300}{T_e}\right)^{4.5}\ cm^6/s$

D9. $O_2^+ + e \rightarrow O + O$ $2.1E(-7)\left(\dfrac{300}{T_e}\right)^{0.7}\ cm^3/s$

D10. $O_4^+ + e \rightarrow O + O + O_2$ $2.0E(-6)\ cm^3/s$

D11. $He^+ + e + e \rightarrow He + e$ $1.0E(-19)\ cm^6/s$

D12. $He_2^+ + e \rightarrow He + He$ $1.0E(-8)\ cm^3/s$

D13. $He_2^+ + e + He \rightarrow 3He$ $2.0E(-27)\ cm^6/s$

D14. $NO^+ + e + e \rightarrow NO + e$ $7.0E(-20)\left(\dfrac{300}{T_e}\right)^{4.5}\ cm^6/s$

D15. $NO^+ + e \rightarrow N + O$ $4.0E(-7)\left(\dfrac{300}{T_e}\right)^{0.4}\ cm^3/s$

D16. $H_3C^+ + e + e \rightarrow H_2O + H + e$ $7.0E(-20)\left(\dfrac{300}{T_e}\right)^{4.5}\ cm^6/s$

D17. $H_3O^+ + e \rightarrow H_2O + H$ $1.3E(-6)\left(\dfrac{300}{T_e}\right)^{1.0}\ cm^3/s$

D18. $O_2^+ \cdot H_2O + e \rightarrow O_2 + H_2O$ $1.5E(-6)\left(\dfrac{300}{T_e}\right)^{0.2}\ cm^3/s$

D19. $H_3O^+ \cdot OH + e + e \rightarrow H_2O + OH + H + e$ $7.0E(-20)\left(\dfrac{300}{T_e}\right)^{4.5}\ cm^6/s$

D20. $H_3O^+ \cdot OH + e \rightarrow H_2O + OH + H$ $2.0E(-6)\left(\dfrac{300}{T_e}\right)^{0.2}\ cm^3/s$

D21. $H_3O^+ \cdot H_2O + e + e \rightarrow 2H_2O + H + e$ $7.0E(-20)\left(\dfrac{300}{T_e}\right)^{4.5}$ cm^6/s

D22. $H_3O^+ \cdot H_2O + e \rightarrow 2H_2O + H$ $2.8E(-6)\left(\dfrac{300}{T_e}\right)^{0.15}$ cm^3/s
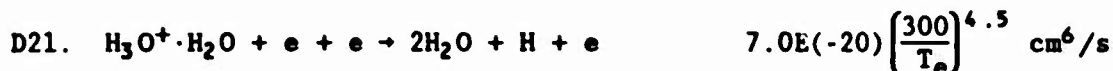
E. TWO-BODY POSITIVE-ION NEGATIVE-ION RECOMBINATION

Reaction	Rate
E1. $N^+ + O^- \rightarrow N + O$	$2.6E(-7)\left(\dfrac{300}{T_{air}}\right)^{0.5}$ cm^3/s
E2. $N_2^+ + O_2^- \rightarrow N_2 + O_2$	$1.6E(-7)\left(\dfrac{300}{T_{air}}\right)^{0.5}$ cm^3/s
E3. $O^+ + O^- \rightarrow O + O$	$2.7E(-7)\left(\dfrac{300}{T_{air}}\right)^{0.5}$ cm^3/s
E4. $O_2^+ + O^- \rightarrow O_2 + O$	$1.0E(-7)\left(\dfrac{300}{T_{air}}\right)^{0.5}$ cm^3/s
E5. $O_2^+ + O_2^- \rightarrow O_2 + O_2$	$4.2E(-7)\left(\dfrac{300}{T_{air}}\right)^{0.5}$ cm^3/s
E6. $NO^+ + O^- \rightarrow NO + O$	$4.9E(-7)\left(\dfrac{300}{T_{air}}\right)^{0.5}$ cm^3/s
E7. $NO^+ + O_2^- \rightarrow NO + O_2$	$6.0E(-7)\left(\dfrac{300}{T_{air}}\right)^{0.5}$ cm^3/s

F. THREE-BODY CLUSTER-ION RECOMBINATION

An estimate for the three-body cluster-ion recombination rate is

$$1.0E(-25)\left(\dfrac{300}{T_{air}}\right)^{2.5} \text{ cm}^6\text{/s}$$

where the third body is N_2 (the dominant air species). Little information is available for individual reactions, hence, the reaction rate for the following reaction are all the same.

F1. $O_2^+ + O_3^- + N_2 \rightarrow 2O_2 + O + N_2$

F2. $O_2^+ + O_4^- + N_2 \rightarrow 3O_2 + N_2$

F3. $O_2^+ + CO_3^- + N_2 \rightarrow O_2 + CO_2 + O + N_2$

F4. $O_2^+ + CO_4^- + N_2 \rightarrow 2O_2 + CO_2 + N_2$

F5. $O_2^+ + O_2^- \cdot H_2O + N_2 \rightarrow 2O_2 + H_2O + N_2$

F6. $O_4^+ + O^- + N_2 \rightarrow 2O_2 + O + N_2$

F7. $O_4^+ + O_2^- + N_2 \rightarrow 3O_2 + N_2$

F8. $O_4^+ + O_3^- + N_2 \rightarrow 2O_2 + O_3 + N_2$

F9. $O_4^+ + O_4^- + N_2 \rightarrow 4O_2 + N_2$

F10. $NO^+ + O_3^- + N_2 \rightarrow NO + O_2 + O + N_2$

F11. $NO^+ + O_4^- + N_2 \rightarrow NO + 2O_2 + N_2$

F12. $NO^+ + CO_3^- + N_2 \rightarrow NO + CO_2 + O + N_2$

F13. $NO^+ + CO_4^- + N_2 \rightarrow NO + CO_2 + O_2 + N_2$

F14. $NO^+ + O_2^- \cdot H_2O + N_2 \rightarrow NO + H_2O + O + N_2$

F15. $NO^+ + CO_3^- \cdot H_2O + N_2 \rightarrow NO + H_2O + CO_2 + O + N_2$

F16. $NO^+ + CO_4^- \cdot H_2O + N_2 \rightarrow NO + H_2O + CO_2 + O_2 + N_2$

F17. $O_2^+ \cdot H_2O + O^- + N_2 \rightarrow O_2 + H_2O + O + N_2$

F18. $O_2^+ \cdot H_2O + O_2^- + N_2 \rightarrow 2O_2 + H_2O + N_2$

F19. $O_2^+ \cdot H_2O + O_3^- + N_2 \rightarrow O_2 + O_3 + H_2O + N_2$

F20. $O_2^+ \cdot H_2O + CO_3^- + N_2 \rightarrow O_2 + O + H_2O + CO_2 + N_2$

F21. $O_2^+ \cdot H_2O + CO_4^- + N_2 \rightarrow 2O_2 + H_2O + CO_2 + N_2$

F22. $O_2^+ \cdot H_2O + O_2^- \cdot H_2O + N_2 \rightarrow 2O_2 + 2H_2O + N_2$

F23. $H_3O^+ \cdot H_2O + O^- + N_2 \rightarrow 2H_2O + OH + N_2$

F24. $H_3O^+ \cdot H_2O + O_2^- + N_2 \rightarrow 2H_2O + OH + O + N_2$

F25. $H_3O^+ \cdot H_2O + O_3^- + N_2 \rightarrow 2H_2O + OH + O_2 + N_2$

F26. $H_3O^+ \cdot H_2O + O_4^- + N_2 \rightarrow 2H_2O + OH + O_3 + N_2$

F27. $H_3O^+ \cdot H_2O + CO_3^- + N_2 \rightarrow 2H_2O + OH + CO_2 + N_2$

F28. $H_3O^+ \cdot H_2O + CO_4^- + N_2 \rightarrow 2H_2O + OH + CO_2 + O + N_2$

F29. $H_3O^+ \cdot H_2O + O_2^- \cdot H_2O + N_2 \rightarrow 3H_2O + OH + O + N_2$

F30. $H_3O^+ \cdot H_2O + CO_3^- \cdot H_2O + N_2 \rightarrow 3H_2O + OH + CO_2 + N_2$

F31. $H_3O^+ \cdot H_2O + CO_4^- \cdot H_2O + N_2 \rightarrow 3H_2O + OH + CO_2 + O + N_2$

Appendix B

IONIZATION PRODUCTS AND MASS ATTENUATION COEFFICIENTS

Appendix B

IONIZATION PRODUCTS AND MASS ATTENUATION COEFFICIENTS

Reference 12 provides a theoretical estimate of the particle production rate of air bombarded by betas, X-rays, or gammas. These 1974 estimates are approximate and reflect accuracies of ±5 percent for N_2^+ and O_2^+; ±20 percent for N^+, O^+, N, and N*; and ±30 percent for the other neutrals. Table B-1 is the production rate table derived from the 1974 computational model ISRAD in Reference 12.

Table B.1

SPECIES PRODUCTION RATES

Species	Particles per Ion Pair*
$N_2^+(X^2\Sigma_g^+)$	0.63
$N^+(^3P)$	0.14
$N_2(A^3\Sigma_u^+)$	0.53
$N_2(a^1\Pi_g)$	0.11
$N(^4S^\circ)$	0.50
$N(^2D^\circ) + N(^2P^\circ)$	0.51
$O_2^+(X^2\Pi_g) + O_2^+(a^4\Pi_u)$	0.16
$O^+(^4S^\circ)$	0.07
$O^-(^2P)$	0.02
$O(^3P)$	0.21
$O(^1D) + O(^1S)$	0.12
$O_2(a^1\Delta_g)$	0.78
$O_2(b^1\Sigma_g^+)$	0.12

*Bombardment of dry air with betas, X-rays, or gammas.

The mean range of an ionization source, r_m, is given by

$$r_m = \frac{1}{\left[\frac{\mu_o}{\rho_o}\right]\rho} \qquad , \qquad (B.1)$$

where μ_o/ρ_o (in cm^2/g) is the mass attenuation coefficient for ionization processes and ρ (in g/cm^3) is the mass density of the medium. The mass attenuation coefficient in Table B.2 were extracted from Pages et al.[*] and Evans.[†]

---

[*]L. Pages, E. Bertel, H. Joffre, and L. Sklavenitis, "Energy Loss, Range, and Bremsstrahlung Yield for 10-KeV to 100-KeV Electrons," Atomic Data, Vol. 4, pp. 1-127 (1972).

[†]R. D. Evans, The Atomic Nucleus, pp. 672-746 (McGraw-Hill, New York, NY, 1955).

Table B.2

MASS ATTENUATION COEFFICIENTS

Energy (KeV)	μ_0/ρ_0 in cm^2/g		
	Photons in Air	Electrons in Air	Electrons in Helium
10	4.1	3.94×10^3	4.44×10^3
15	1.3	1.81×10^3	2.03×10^3
20	4.8×10^{-1}	1.06×10^3	1.19×10^3
30	1.4×10^{-1}	5.08×10^2	5.65×10^2
40	6.0×10^{-2}	3.04×10^2	3.37×10^2
50	3.8×10^{-2}	2.04×10^2	2.26×10^2
60	2.8×10^{-2}	1.49×10^2	1.64×10^2
70	2.5×10^{-2}	1.14×10^2	1.25×10^2
80	2.4×10^{-2}	9.01×10^1	9.90×10^1
90	2.4×10^{-2}	7.35×10^1	8.13×10^1
100	2.4×10^{-2}	6.17×10^1	6.76×10^1
150	2.5×10^{-2}	3.13×10^1	3.42×10^1
200	2.7×10^{-2}	1.97×10^1	2.14×10^1
300	2.8×10^{-2}	1.05×10^1	1.14×10^1
400	2.9×10^{-2}	6.90	7.41
500	3.0×10^{-2}	5.03	5.41
600	2.9×10^{-2}	3.91	4.20
700	2.9×10^{-2}	3.19	3.41
800	2.8×10^{-2}	2.69	2.87
900	2.7×10^{-2}	2.32	2.48
1,000	2.7×10^{-2}	2.04	2.17
2,000	2.4×10^{-2}	9.26×10^{-1}	9.80×10^{-1}
3,000	2.1×10^{-2}	6.06×10^{-1}	6.37×10^{-1}
4,000	1.9×10^{-2}	4.55×10^{-1}	4.76×10^{-1}
5,000	1.8×10^{-2}	3.66×10^{-1}	3.82×10^{-1}

Data: Densities at stp--dry air, 1.29×10^{-3} g/cm^3;
helium, 1.77×10^{-4} g/cm^3.

Appendix C
HELIUM INVENTION DISCLOSURE

Title of Invention: BROADBAND ELECTROMAGNETIC ABSORPTION VIA A COLLISIONAL HELIUM PLASMA

Date of Conception: 10 May 1983

Date of First Drawing, Sketch, Model: 9 May 1986

   Presently Available at:

Date of First Disclosure to Others: 9 May 1986   **To Whom:** Donald J. Eckstrom

Date First Successfully Made or Used   **Where:**

Date or Anticipated Date of First Public Disclosure:

   Where and How:

Invention Conceived and/or Reduced to Practice in Performance of:

   Government Prime Contract or Subcontract No. F49620-85-K-0013 15 May 1985 to 14 Jan 1987

   Commercial Prime Contract or Subcontract No.

   SRI-Sponsored Project No. IR&D LLA 9 Jan 1984 to 30 April 1984

   Grant No.

   Other (specify) Vidmar: 160 Hours, non-compensated, in preliminary research from
          10 May 1983 to 9 Jan 1984

Inventor(s):

1.   Robert J. Vidmar

         Print Name   Signature   Date

   Box 2207, Stanford, CA 94305

           Residence (include street, city, state and zip code)

2.

         Print Name   Signature   Date

           Residence (include street, city, state and zip code)

3.

         Print Name   Signature   Date

           Residence (include street, city, state and zip code)

4.

         Print Name   Signature   Date

           Residence (include street, city, state and zip code)

Witnessed and understood by me:

                               Signature   Date

SRI 1011 (7/77)

Present Location of Drawings, Sketches, Reports, Notebooks, etc.:

SRI International, 320T5-7

Advantages of Invention:

The absorptive helium plasma is a broadband absorber of electromagnetic waves. It has a bandwidth for absorption of at least 6 octaves. The frequency band for absorption depends on the plasma frequency and the degree of absorption depends on the electron-helium collision rate. Calculations that utilize helium as the working gas indicate the power required to generate the plasma is of the order of 500 W/m^3.

Prior Art (most pertinent publications, patents and practices, and how invention differs therefrom:

Use of Invention (extent of use, e.g., laboratory, pilot plant, commercial; if not used, is use likely or contemplated, and when):

The absorptive helium plasma could be utilized in conjunction with a radar antenna installed in a ground-based or airborne radome for the following purposes: (1) suppress sidelobe emissions during transmission, (2) reduce sidelobe noise during reception, and (3) reduce radar antenna backscatter.

Inventor(s):

1. _____ _____
   Signature   Date

2. _____ _____
   Signature   Date

3. _____ _____
   Signature   Date

4. _____ _____
   Signature   Date

Witnessed and understood by me: _____
                                 Signature   Date

40

Detailed Description of Invention (additional pages of description and/or drawings <u>must</u> be signed, dated and witnessed as is this page):

A collisional plasma absorbs energy from an electromagnetic wave via electron-neutral momentum-transfer collisions. If the momentum-transfer collision rate provides several collisions during each cycle of an electromagnetic wave, then some of the energy transferred to electrons from the wave heats the neutral gas and is lost. The helium plasma is unique in that it has the lowest electron-ion recombination rate for gases and does not suffer from accelerated recombination due to dimer or trimer ion formation. A helium plasma with an electron density of 6×10^{16} m^{-3} operating at a fraction of atmospheric pressure with a collision rate of $\sim 40 \times 10^9$ s^{-1}, can attenuate waves from 30 MHz to 10 GHz. Preliminary calculations indicate attenuation of the order of 20 dB per meter and power to maintain this plasma is of the order of 500 W/m^3. The mechanism to generate the plasma is an electron beam with an energy of the order of 100 keV and a beam current of the order of 5 mA per cubic meter of helium plasma.

Inventor(s):

1. _____
   Signature   Date

2. _____
   Signature   Date

3. _____
   Signature   Date

4. _____
   Signature   Date

Witnessed and understood by me:_____
                                        Signature   Date

REFERENCES

1. J. S. Chang and W. H. Duewer, "Modeling Chemical Processes in the Stratosphere," Ann. Rev. Phys. Chem., Vol. 30, pp. 443-469 (1979).

2. R. D. Hudson and L. J. Kieffer, "Compilation of Atomic Ultraviolet Photoabsorption Cross Sections for Wavelengths between 3000 and 10 Å," Atomic Data, Vol. 2, pp. 205-262 (1971).

3. J. H. Hubbell, "Survey of Photon-Attenuation--Coefficient Measurements 10 eV to 100 GeV," Atomic Data, Vol. 3, pp. 241-297 (1971).

4. Radiological Health Handbook, Revised Edition, pp. 458, (U.S. Department of Health, Education, and Welfare, 1970).

5. L. Pages, E. Bertel, H. Joffre, and L. Sklavenitis, "Energy Loss, Range, and Bremsstrahlung Yield for 10-KeV to 100-MeV Electrons," Atomic Data, Vol. 4, pp. 1-127 (1972).

6. American Institute of Physics Handbook, 3rd Ed., p. 8-184 and 8-296 (McGraw-Hill, New York, NY, 1982).

7. R. E. Bolz and G. L. Tuve, Handbook of Tables for Applied Engineering Science, 2nd Ed. (CRC Press, 1983).

8. M. H. Bortner and T. Bauer, Defense Nuclear Agency Reaction Rate Handbook, 2nd Ed. (DASIAC, Santa Barbara, CA, 1972).

9. B. Tanenbaum, Plasma Physics, pp. 246-252, (McGraw-Hill, New York, NY, 1967).

10. K. Liou, An Introduction to Atmospheric Radiation, pp. 50-52 (Academic Press, New York, NY, 1980).

11. L. G. Christophorou, Electron-Molecule Interactions and Their Applications, Volume 2, pp. 72-82 (Academic Press, New York, NY, 1984).

12. "Electron Energy Degradation in the Atmosphere: Consequent Species and Energy Densities, Electron-Flus, and Radiation Spectra, Topical Report DNA 3513T, Contract No. DNA001-74-C-0149 (1974).

13. R. V. Hodges, L. C. Lee, and J. T. Moseley, "Photo Dissociation and Photodetachment of Molecular Negative Ions. IX. Atmospheric Ions at 2484 and 3511 Å," J. Chem. Phys., Vol. 72, pp. 2998-3000 (1980).

14. T. J. Dwyer, J. R. Greig, D. P. Murphy, J. M. Perin, R. E. Pechacek, and M. Raleigh, "On the Feasibility of Using an Atmospheric Discharge Plasma as an RF Antenna," IEEE Antennas and Propagation, Vol. AP-32, No. 2, pp. 141-146, (1984).

15. R. D. Evans, The Atomic Nucleus, pp. 672-746 (McGraw-Hill, New York, NY, 1955).